Available online at www.sciencedirect.com
ScienceDirect
Advances in Space Research 39 (2007) 315–323
ADVANCES IN SPACE RESEARCH (a COSPAR publication)
www.elsevier.com/locate/asr

Calibration of MICROSCOPE

E. Guiu *, M. Rodrigues, P. Touboul, G. Pradels [1]

Office National d'Études et de Recherches Aérospatiales, Physics and Instrumentation Department, BP 72, 92320 Châtillon, France

Received 15 November 2004; received in revised form 20 June 2006; accepted 21 June 2006

Abstract

The MICROSCOPE mission is planned for launch in early 2009. It aims to verify the Equivalence Principle to an accuracy of 10^{-15}, which is currently difficult to obtain on Earth because of the intrinsic limitations of the torsion pendulum and disturbing phenomena, like seismic activity. In space the experiment can take advantage of the quiet environment provided by a drag-free satellite.

The instrument used for the test is a differential electrostatic accelerometer composed of two inertial sensors with test-masses made of different materials: one in Platinum–Rhodium alloy, the other in Titanium alloy. The space experiment will also benefit from a second differential accelerometer with both test-masses of the same material, which will be used as a reference instrument to characterise the disturbing signals and sensitivities.

The in-orbit calibration of the instrument is mandatory to validate the space test and several procedures have been previously proposed, taking advantage of the satellite propulsion system or the a priori knowledge of natural in-orbit applied accelerations. Due to the actual configuration of the MICROSCOPE propulsion system, the possibility of accurate satellite manoeuvres is limited but sufficient. This paper presents the necessary compromise between the knowledge of satellite and instrument parameters and the calibration procedures. The scenario of the MICROSCOPE in-orbit calibration phase is finely defined in agreement with the required performances for the EP test accuracy.

Keywords: Equivalence principle; Calibration; SCAO; Accelerometer; Drag free

1. Introduction

The universality of free fall is one of the most obvious consequences of the Equivalence Principle (EP): two bodies subjected to the same field of gravity undergo the same acceleration, regardless of their dimensions and internal composition. Einstein (Einstein, 1907) expressed the EP principle, empirically known since Galilee and Newton, as a postulate of his theory of general relativity.

Two types of tests on ground have reached accuracies of a few 10^{-13}. One is based on a torsion pendulum experiment with masses of different composition submitted to the same Sun attraction (Baessler et al., 1999). The other consists in years of laser ranging measurement between the Earth and the Moon to survey the relative motion of the two celestial bodies of different compositions (only Earth has an internal iron core) (Nordtvedt, 2003). Nowadays both these experiments are limited by the environment.

The MICROSCOPE microsatellite mission was proposed in 1999 by the ONERA aerospace research institute and the Observatoire de la Côte d'Azur (OCA), and selected by CNES, the French space agency. The primary scientific objective of the mission is the test of the Equivalence Principle to an accuracy of at least 10^{-15}, by comparing the equivalence between the inertial mass and the gravitational mass of two bodies of different composition and density (Touboul et al., 2001).

This improvement in accuracy of at least two orders of magnitude will be achieved by using ultrasensitive

* Corresponding author. Tel.: +33 1 46 73 45 03.
E-mail address: emeline.guiu@onera.fr (E. Guiu).
[1] On behalf of ONERA from Oct. 2000 to Oct. 2003.

0273-1177/$30
doi:10.1016/j.asr.2006.06.012

electrostatic accelerometers, developed in our laboratory for space applications and by taking advantage of the specific environment and operation of the dedicated satellite.

2. MICROSCOPE

2.1. The mission

MICROSCOPE will be the third microsatellite of the MYRIADE family, developed by CNES since 1996. The first one, DEMETER, was successfully launched in June 2004. Besides its first survey of the Earth electromagnetic emissions linked to seismic phenomena, the mission already demonstrates the performance of the recurring technology for the microsatellite production line. After PARASOL, the second satellite devoted to the characterisation microphysical and radiative properties of clouds and aerosols, launched in December 2004, MICROSCOPE is scheduled to be launched in March 2009 by a Russian Dnepr launcher or equivalent.

The MICROSCOPE satellite will fly at an altitude of 730 km on a quasi-polar and heliosynchronous orbit with a less than 5×10^{-3} eccentricity. It takes advantage of this low eclipse rate orbit to maintain the payload in a very stable thermal environment.

The 200 kg satellite is roughly one cubic meter featuring two deployable solar panels always facing the sun during the mission. The star tracker and mechanical and thermal interface of the payload are fixed on the opposite side of the satellite from the solar panels (Fig. 1). The two lateral sides carry four pods of three electrical thrusters used for the satellite attitude and orbit control.

The MICROSCOPE satellite includes an original drag-free control system which compensates for the applied surface forces, such as solar pressure and residual atmosphere drag which deviate the orbit from a purely gravitational one. The actuation of the thrusters is based on the measurements delivered by the payload accelerometers and the star tracker. Both angular and translational satellite motions are finely controlled to reduce the accelerations applied on the instrument, and thus decrease the environmental noise. The attitude and drag-free control will control the motion of the satellite to levels as low as $3 \times 10^{-10}\ \mathrm{m\,s^{-2}}/\sqrt{\mathrm{Hz}}$. This system also allows a precise spin rate to be applied or not: if the satellite is not spun, it is in quasi-inertial pointing mode.

2.2. The science instrument SAGE

The two differential accelerometers (Fig. 2) of the payload fulfill two functions simultaneously: as the science payload devoted to and optimized for the EP test, and as the inertial reference sensor for the drag-free and attitude control of the satellite. Each accelerometer contains two cylindrical and concentric test-masses, one instrument with masses of different materials to be compared in free fall, the other with two masses of the same material to evaluate stochastic and systematic errors (Touboul and Rodrigues, 2001). The center of masses of each differential accelerometer and the center of mass of the satellite are aligned in order to minimize the effects of attitude and the power necessary to nullify the drag. The alignment of the center of masses also attenuates the effect of the satellite spin on the accelerometer measurement.

In the case of an EP violation, the test-masses of each accelerometer, when free, will not follow the same in-orbit gravitational trajectory. The weak electrostatic forces generated to keep both test-masses on the same orbit will be accurately measured in the MICROSCOPE instrument. A difference of applied acceleration gives potential evidence of a violation of the EP.

The acceleration of the satellite depends on the non-gravitational forces $\overrightarrow{F_{\mathrm{ng}}}$ and the acceleration induced by the Earth's gravity field, simply expressed by

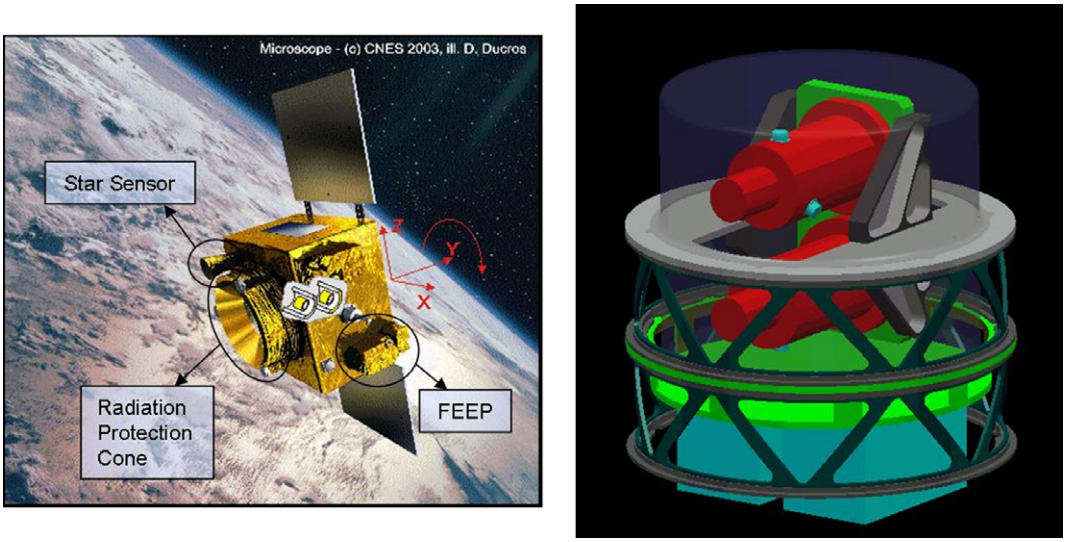

Fig. 1. Position of the instruments in the satellite.

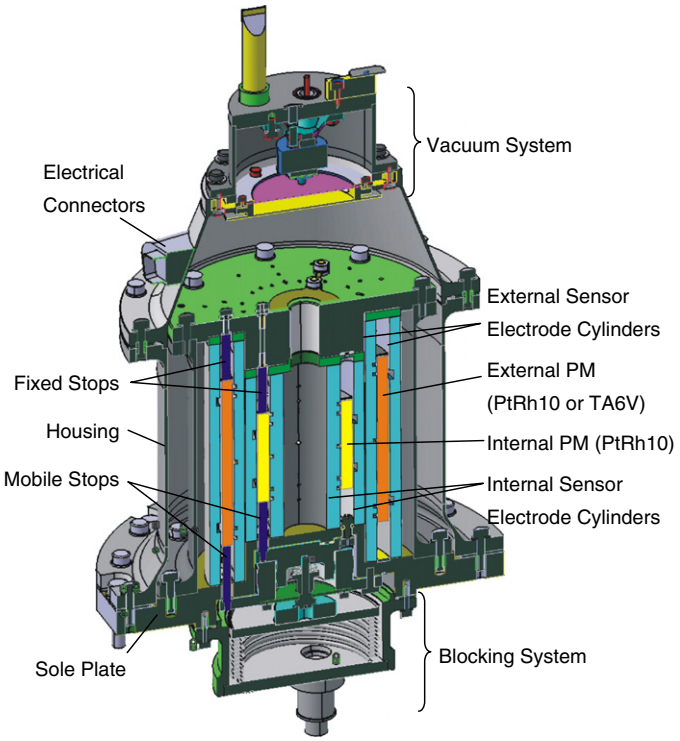

Fig. 2. Configuration of one differential accelerometer.

$$\overrightarrow{\Gamma}(O_{\text{sat}}) = \frac{\overrightarrow{F_{\text{ng}}}}{m_{\text{sat,I}}} + \frac{m_{\text{sat,g}}}{m_{\text{sat,I}}} \cdot \overrightarrow{g}(O_{\text{sat}}), \tag{1}$$

where $m_{\text{sat,g}}$ represents the gravitational mass of the satellite, $m_{\text{sat,I}}$ its inertial mass and $\overrightarrow{g}(O_{\text{sat}})$ the Earth's gravity field at the satellite centre of gravity O_{sat}.

The measured acceleration of the test-mass (denoted by the index $k = 1$ for internal and $k = 2$ for external) depends on the electrostatic acceleration applied onto the mass to control its motion, $\overrightarrow{\Gamma}_{\text{app},k}$, and on the gravity field at its center $\overrightarrow{g}(O_k)$. The mass is considered here as a monopole with respect to the Earth's field. Then, in the case of a perfect instrument, one has

$$\overrightarrow{\Gamma}_{\text{app},k} = \overrightarrow{\Gamma}(O_k) - \frac{m_{gk}}{m_{\text{I}k}} \cdot \overrightarrow{g}(O_k) \tag{2}$$

with m_{gk} representing the gravitational mass of the test-mass k and $m_{\text{I}k}$ its inertial mass.

- $\overrightarrow{\Gamma}(O_k) = \overrightarrow{\Gamma}(O_{\text{sat}}) - [In] \cdot \overrightarrow{O_kO}_{\text{sat}} - 2 \cdot [Cor] \cdot \dot{\overrightarrow{O_kO}}_{\text{sat}} - \ddot{\overrightarrow{O_kO}}_{\text{sat}}$ and
- $\overrightarrow{g}(O_k) = \overrightarrow{g}(O_{\text{sat}}) + [T] \cdot \overrightarrow{O_kO}_{\text{sat}}$.

Combining Eqs. (1) and (2) gives

$$\overrightarrow{\Gamma}_{\text{app},k} = \frac{\overrightarrow{F}_{\text{ng}}}{m_{\text{sat,I}}} + \left(\frac{m_{\text{sat,g}}}{m_{\text{sat,I}}} - \frac{m_{gk}}{m_{\text{I}k}}\right) \cdot \overrightarrow{g}(O_{\text{sat}}) + ([T] - [In]) \cdot \overrightarrow{O_kO}_{\text{sat}} - 2 \cdot [Cor] \cdot \dot{\overrightarrow{O_kO}}_{\text{sat}} - \ddot{\overrightarrow{O_kO}}_{\text{sat}}, \tag{3}$$

when linearizing the Earth's gravity variations expressed with the gravity gradient tensor $[T]$, with the inertial tensor $[In]$ representing the sum of the angular and centrifugal accelerations and $[Cor]$ representing the Coriolis effect. In the following each variable in square bracket is a 3×3 tensor.

The terms $2 \cdot [Cor] \cdot \dot{\overrightarrow{O_kO}}_{\text{sat}}$ and $\ddot{\overrightarrow{O_kO}}_{\text{sat}}$ are negligible because of the stability of the distance O_k $_{\text{Osat}}$.

Pointing, angular velocity and acceleration are specified so that the inertial tensor $[In]$ ($In_{ij} \simeq 10^{-11}\ \text{s}^{-2}$ with $\{i,j\} \in \{x,y,z\}$ the three instrument reference axes) is negligible with respect to the gravity tensor $[T]$ at the frequency of the test f_{ep} ($T_{ij} \leqslant 4 \times 10^{-9}\ \text{s}^{-2}$) and frequencies of calibration ($T_{ij} \leqslant 10^{-6}\ \text{s}^{-2}$ at $2 \cdot f_{\text{orb}}$).

The gravity gradient $[T]$ is obtained by a double derivation of the Earth's gravity potential U: $[T] = \overrightarrow{\nabla}(\overrightarrow{\nabla}(U))$.

$$T_{ij} = \frac{\partial^2 U}{\partial x_i \partial x_j} = \frac{\partial^2 U}{\partial x_j \partial x_i} = T_{ji}.$$

The gravity gradient matrix is symmetrical (Touboul et al., 2001).

The half difference between the applied accelerations on the two masses of one differential accelerometer

$$\overrightarrow{\Gamma}_{\text{app},d} = \tfrac{1}{2} \cdot (\overrightarrow{\Gamma}_{\text{app},1} - \overrightarrow{\Gamma}_{\text{app},2})$$

leads to

$$\overrightarrow{\Gamma}_{\text{app},d} \approx 1/2 \cdot (\delta \cdot \overrightarrow{g}(O_{\text{sat}}) + [T] \cdot \overrightarrow{\Delta}), \tag{4}$$

where $\delta = \frac{m_{g2}}{m_{I2}} - \frac{m_{g1}}{m_{I1}} \simeq \eta$ is the EP signal, η being the Eötvös ratio ((Dittus and Mehls, 2001)). $\overrightarrow{\Delta} = \overrightarrow{O_1O_2}$ is the offcentring between the two test-masses and is fixed by the instrument structure stability and by the instrument operation to control the masses motionless with respect to the structure.

The Eötvös ratio represents the potential EP violation signal which will be at the orbital frequency when the mass axes are inertial pointing. This differential acceleration, $\overrightarrow{\Gamma}_{\text{app,d}}$, is the science measurement data, in which the EP signal is coupled to the effect of the gravity gradient and the inertial accelerations when the two considered bodies are not centred.

The half sum of the accelerations, $\overrightarrow{\Gamma}_{\text{app},c}$, is defined in a similar way:

$$\overrightarrow{\Gamma}_{\text{app},c} = \tfrac{1}{2}\cdot(\overrightarrow{\Gamma}_{\text{app},1} + \overrightarrow{\Gamma}_{\text{app},2}).$$

$$\overrightarrow{\Gamma}_{\text{app},c} \approx \frac{\overrightarrow{F}_{\text{ng}}}{m_{\text{sat,I}}} + \left(\frac{m_{\text{sat,g}}}{m_{\text{sat,I}}} - \frac{1}{2}\cdot\left(\frac{m_{g1}}{m_{I1}} + \frac{m_{g2}}{m_{I2}}\right)\right)\cdot\overrightarrow{g}(O_{\text{sat}}) + \frac{1}{2}\cdot[T]\cdot(\overrightarrow{O_1O}_{\text{sat}} + \overrightarrow{O_2O}_{\text{sat}}) \quad (5)$$

This common applied acceleration is fully rejected in the perfect differential measurement expressed in Eq. (4) but any source of sensor axis misalignment or sensitivity mismatching has to be corrected in flight or will partially introduce the acceleration present in Eq. (8). In the following section we will analyze how the instrument defects will be characterized, evaluated in orbit and how the data on ground will be corrected.

3. The MICROSCOPE measurement

In laboratory, the SAGE instrument can not operate under one g and exhibit the expected in-orbit accuracy. Femtog accuracy, after data processing, is expected thanks to a specific design optimized for in-orbit operation with a limited full range of 0.1 μg. The instrument noise level in orbit is 10^{-12} m s$^{-2}/\sqrt{\text{Hz}}$: each sensor has a dynamic range of 10^6. Therefore it is necessary to measure the signal during at least 20 orbits to reject the noise to a sufficient level to achieve the required accuracy of 8×10^{-15} m s^{-2} for the differential measured acceleration.

Specific electronics can be used to levitate the mass on ground but the operation is very different from in orbit and coupling between the vertical axis and the two horizontal axes prevents characterization of the instrument sensitivity and axes orientation with a sufficient accuracy. Furthermore, ground tests of this type of sensor in a controlled horizontal plane are limited by the one g projection that may fluctuate: a 1 ng variation corresponds to a 2×10^{-4} arcsec instability. Thermal fluctuations and human activities may add other sources of error as well. Very accurate measurements have been published by the LISA team (Anza et al., 2005) to levels of a few 10^{-13} m s$^{-2}/\sqrt{\text{Hz}}$ in differential acceleration noise with a torsion pendulum apparatus for the LISA pathfinder mission. This device helps to demonstrate the feasibility of measuring very low accelerations and to find upper limits for the parasitic forces acting on the test masses (like electrostatic, thermal and pressure effects...). However, the measurement errors due to the misknowledge of alignments to sufficient accuracy cannot be directly measured on the Flight Model. The sensitivity and the orientation of the sensors will therefore not be sufficiently well known before the in-orbit operations and an in-flight calibration of the experiment is required to ensure the mission performance.

To define the in-orbit calibration, the instrument and satellite procedures, the expected signals to be analyzed and the data processing need to be carefully defined before the launch. The satellite manoeuvres (Fig. 3) are being defined and analyzed in close collaboration with the satellite team of CNES. The calibration signals have been analyzed with tools similar to the EP test data processing on one hand and with simulation tools on the other hand. This work has been carried out in close collaboration with the OCA team. In the case of a perfect instrument the measurement provided by each inertial sensor, $\overrightarrow{\Gamma}_{\text{meas},k}$, equals $\overrightarrow{\Gamma}_{\text{app},k}$. But for a real instrument, $\overrightarrow{\Gamma}_{\text{meas},k}$ can be expressed by

$$\overrightarrow{\Gamma}_{\text{meas},k} \approx \overrightarrow{K}_{0,k} + [M_k]\cdot\overrightarrow{\Gamma}_{\text{app},k} + \sum_{l=x,y,z}\overrightarrow{u}^t_l\cdot([K_{2,k}]\cdot\overrightarrow{\Gamma}_{\text{app},k}\cdot\overrightarrow{\Gamma}^t_{\text{app},k}\cdot\overrightarrow{u}_l)\cdot\overrightarrow{u}_l + \overrightarrow{\Gamma}_{n,k}, \quad (6)$$

where:

- $\overrightarrow{K}_{0,k}$, the bias vector is mainly constant but may vary according to the instrument environment, mainly the thermal environment,
- $[M_k] \approx [I + dM_k]$ at first order, where $[dM_k]$ represents the errors of sensitivity with respect to the unit matrix I, which has to be limited first by the design and the production accuracy, and then by the qualification and verification procedures,

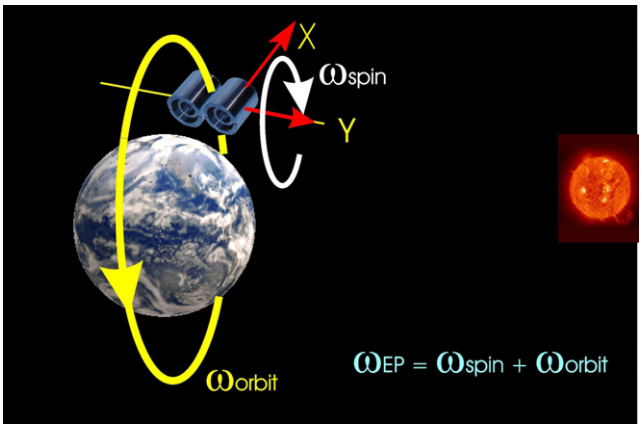

Fig. 3. Instrument axes and orbit.

- $[K_{2,k}]$ is the quadratic sensitivity matrix of the instrument, representing non-linearities of order two: further orders of non-linearities are not considered in the model and all non-linearities are neglected thereafter,
- $\overrightarrow{\Gamma}_{n,k}$ includes all stochastic perturbations.

The differential measured acceleration is then:

$$\overrightarrow{\Gamma}_{\mathrm{meas},d} = \tfrac{1}{2}\cdot(\overrightarrow{\Gamma}_{\mathrm{meas},1} - \overrightarrow{\Gamma}_{\mathrm{meas},2}). \tag{7}$$

By introducing a linear common mode $\overrightarrow{\Gamma}_{\mathrm{app},c} = 1/2\cdot(\overrightarrow{\Gamma}_{\mathrm{app},1} + \overrightarrow{\Gamma}_{\mathrm{app},2})$, $\overrightarrow{\Gamma}_{\mathrm{meas},d}$ can be expressed at first order as a combination of common and differential applied accelerations

$$\overrightarrow{\Gamma}_{\mathrm{meas},d} \approx \overrightarrow{K}_{0,d} + [M_c]\cdot\overrightarrow{\Gamma}_{\mathrm{app},d} + [M_d]\cdot\overrightarrow{\Gamma}_{\mathrm{app},c} + \overrightarrow{\Gamma}_{n,d}, \tag{8}$$

with

- $[M_c] = 1/2\cdot([M_1] + [M_2])$,
- $[M_d] = 1/2\cdot([M_1] - [M_2])$,
- $\overrightarrow{K}_{0,d} = 1/2\cdot(\overrightarrow{K}_{0,1} - \overrightarrow{K}_{0,2})$.

The subscript d characterises the differential mode and the subscript c the common one. $\overrightarrow{\Gamma}_{n,d}$ is estimated by the quadratic sum of the decorrelated noise from the two instruments.

Let (x,y,z) be the instrument reference frame: the axis y points towards the sun, x is oriented towards the Earth in the orbital plane when the satellite flies over the equator and z is deduced from the other axes to obtain an orthonormal frame. Let α be the colatitude angle which varies as the satellite travels around the Earth. In this case, the measured acceleration can be expressed as:

$$\begin{aligned}\overrightarrow{\Gamma}_{\mathrm{meas},d} \approx 1/2\cdot \underbrace{\begin{bmatrix} K_{cx} & \theta_{cz} & -\theta_{cy} \\ -\theta_{cz} & K_{cy} & \theta_{cx} \\ \theta_{cy} & -\theta_{cx} & K_{cz}\end{bmatrix}}_{\sim[M_c]} \\ \cdot\left(\underbrace{\begin{bmatrix} T_{xx} & T_{xy} & T_{xz} \\ T_{xy} & T_{yy} & T_{yz} \\ T_{xz} & T_{yz} & T_{zz}\end{bmatrix}}_{[T]}\cdot\underbrace{\begin{vmatrix}\Delta_x \\ \Delta_y \\ \Delta_z\end{vmatrix}}_{\Delta} - \delta\cdot\underbrace{\begin{vmatrix} g\cdot\sin(\alpha) \\ 0 \\ g\cdot\cos(\alpha)\end{vmatrix}}_{\overrightarrow{g}}\right) \\ + [M_d]\cdot\overrightarrow{\Gamma}_{\mathrm{app},c} + \overrightarrow{K}_{0,d} + \overrightarrow{\Gamma}_{n,d}\end{aligned} \tag{9}$$

with $\alpha \approx 2\pi f_{\mathrm{orb}}\cdot t$ for a quasi-circular orbit. θ_{ci} represents the misalignments and the coupling (which is negligible) between the instrument and the satellite reference frame about the i axis and dK_{ci} is the i axis scale factor error. When the satellite travels around the Earth, the colatitude varies. T_{xy} and T_{yz} are neglected because of the orbit low eccentricity and the orientation of the satellite with respect to the Earth.

Eq. (9) shows that the instrument output at f_{orb} gives directly the EP test signal $\delta/2$ if the other terms can be considered negligible at the same frequency and phase. Because the instrument x axis is the most sensitive, it is the only axis to be considered hereafter: it is the science measurement axis.

$$\Gamma_{\mathrm{meas},dx} = \underbrace{(1+dK_{cx})}_{K_{cx}}\cdot T_{xx}(f_{ep})\cdot\Delta_x/2 \rightarrow \text{offcentring along x axis} \tag{10a}$$

$$+K_{cx}\cdot T_{xz}(f_{ep})\cdot\Delta_z/2 \rightarrow \text{offcentring along z axis} \tag{10b}$$

$$+\theta_{cz}\cdot T_{yy}\cdot\Delta_y/2 \rightarrow \text{sensitivity to axis misalignment} \tag{10c}$$

$$+\theta_{cy}\cdot T_{zz}\cdot\Delta_z/2 \rightarrow \text{other axes misalignment} \tag{10d}$$

$$+M_{dx}\cdot\overrightarrow{\Gamma}_{\mathrm{app},c} \rightarrow \text{differential disturbing terms} \tag{10e}$$

$$+K_{0,dx} \rightarrow \text{bias} \tag{10f}$$

$$+\Gamma_{n,dx} \rightarrow \text{noise} \tag{10g}$$

$$-(K_{cx}\cdot g\cdot\sin(\alpha) - \theta_{cy}\cdot g\cdot\cos(\alpha))\cdot\delta/2 \rightarrow \text{signal to be detected} \tag{10h}$$

The common disturbing terms represent the misalignments between the instrument sensitive axis and the satellite reference frame. The differential disturbing terms represent misalignments and mismatchings between the two sensor axes of the instrument.

$M_{dx} = [K_{dx},\theta_{dy},\theta_{dz}]$ represents the first line of the differential sensitivity matrix with the difference of the sensor sensitivities limited to 10^{-2} and the misalignment limited to 1.5×10^{-3} rad by design. $[M_d]$ is constructed in the same way as the common matrix, $[M_c]$ and is the rejection of the common mode. The error on the differential and common scale factors is maximised: $|K_{cx}| = |K_{dx}| = |K_{1x}| = |K_{2x}| \leqslant 10^{-2}$. The differential acceleration is deduced from the acceleration of each sensor.

The terms composing $\Gamma_{\mathrm{meas},dx}$ disturb at the same frequency as the signal to be detected, $K_{cx}\cdot\delta\cdot g\cdot\sin(\alpha)/2$. They are thus either limited by design, or will be corrected after evaluation.

For the sensitivity matrices and the defects, three types of performance strategies are linked:

- specify the parameters (inertia, acceleration environment…) to be sufficiently low with respect to the EP performance objective,
- estimate the parameters (offcentring) to correct the measurement,
- improve the knowledge of the parameters (alignment) to reduce the effect of the disturbances.

4. Before calibration

The $\delta g/2$ signal to be detected in Eq. (10) has an amplitude of about $4\times10^{-15}\,\mathrm{m\,s^{-2}}$ (for an altitude of 730 km and a EP violation at about 10^{-15}). The MICROSCOPE mission being specified for a signal to noise ratio of 1, the accuracy required for the differential measurement is of the same amplitude $4\times10^{-15}\,\mathrm{m\,s^{-2}}$. All the disturbing terms of Eq. (10) must therefore be estimated or reduced down to a certain amplitude. The approach chosen to specify a uniform value for each term: a disturbing amplitude of $10^{-16}\,\mathrm{m\,s^{-2}}$ has been allocated considering a number of 40 terms.

It is first mandatory to evaluate each disturbing term with respect to the expected accuracy measurement for the EP test. Long-term variations of the calibrated

parameters have been theoretically calculated to specify how often they have to be calibrated (about every 3 months).

The $\delta/2$ term to be recovered (in Eq. 10h) is corrupted by the instrument scale factor inaccuracies dK_{cx}, fortunately limited by design to less than 10^{-2}, that will only limit the accuracy of the δ estimation but not the sensitivity. $\theta_{cy} \cdot \cos(\alpha)$ is rejected because of the limited error angle θ_{cy} and because it is in quadrature.

The bias $K_{0,dx}$ (Eq. 10f) does not need to be calibrated as it gives a DC signal. Thermal variations of the bias and of other parameters do not disrupt the calibration. Variation of the bias is considered in the global error budget for the EP test and limited by specification of the system.

Only potential fluctuations at the same frequency as α variations shall have to be limited by design and operation conditions, as well as the $\Gamma_{n,dx}$ term. Their spectral densities are specified around the EP signal frequency to less than 10^{-12} m s$^{-2}/\sqrt{\text{Hz}}$ for agreement with the 20 orbit minimum duration of each experimental measurement of the Equivalence Principle.

The centres of gravity of the test-masses cannot be perfectly merged. By construction, the maximum separation between them is 20 μm and this distance cannot be controlled and known better than this value during the instrument operation. This offcentring is the main contributor to the disturbing measurement.

This contribution occurs in the terms $K_{cx} \cdot T_{xx}(f_{ep}) \cdot \Delta_x/2$ and $K_{cx} \cdot T_{xz}(f_{ep}) \cdot \Delta_z/2$ (Eqs. (10a) and (10b)). Before calibration, $\Delta_x \approx \Delta_z \leqslant 20 \times 10^{-6}$ m. The scale factor K_{cx} is not calibrated and is known a priori to $\pm 10^{-2}$. The orbit eccentricity e is specified to less than 5×10^{-3} and therefore the gravity gradients are at the order of $T_{xx}(f_{ep}) \approx T_{xz}(f_{ep}) \approx 4.15 \times 10^{-9}$ s^{-2}. The error can then be estimated as:

- $K_{cx} \cdot T_{xx}(f_{ep}) \cdot \Delta_x/2 \leqslant 4.15 \times 10^{-14}$ m s^{-2},
- $T_{xx}(f_{ep}) \cdot \Delta_x/2 \leqslant 4.15 \times 10^{-14}$ m s^{-2},
- $T_{xz}(f_{ep}) \cdot \Delta_z/2 \leqslant 4.15 \times 10^{-14}$ m s^{-2},

which is more than 10 times higher than the signal to be detected without taking into account the other disturbing terms. The aim of the calibration is to reduce the impact of this term on the measurement by a factor 200 using an in-flight estimation of $K_{cx} \cdot \Delta_x$ and $K_{cx} \cdot \Delta_z$. The principle of this estimation is detailed in the following section.

The common sensitivity matrix, M_c, represents the defects of the instrument with respect to satellite reference frame. θ_{ci}, limited to 1.5×10^{-3} rad by construction, represents the angle between the i axis of the instrument and the i axis of the satellite reference frame, based on the star tracker data. This value is due to the alignment error between the accelerometer and the star tracker and to the error in the measurements of the star tracker referred to the inertial reference frame.

$\theta_{cz} \cdot T_{yy} \cdot \Delta_y/2$ is a source of perturbation whose impact has to be evaluated in order to specify both θ_{cz} and Δ_y. Before calibration, $\Delta_y \leqslant 20$ μm, $T_{yy}(f_{ep}) \approx 1.7 \times 10^{-8}$ s^{-2} and $\theta_{cz} \leqslant 1.5 \times 10^{-3}$ rad. $\theta_{cz} \cdot T_{yy} \cdot \Delta_y/2$ (10c) is then limited by design to

$$\theta_{cz} \cdot T_{yy} \cdot \Delta_y/2 \leqslant 2.6 \times 10^{-16} \text{ m s}^{-2}.$$

In the same way $T_{zz}(f_{ep}) \approx 1.3 \times 10^{-8}$ s^{-2} and so $\theta_{cy} \cdot T_{zz} \cdot \Delta_z/2$ (Eq. 10d) is limited to

$$\theta_{cy} \cdot T_{zz} \cdot \Delta_z/2 \leqslant 2 \times 10^{-16} \text{ m s}^{-2},$$

Both contributions are inferior to the signal to be detected but they have to be reduced nonetheless when considering all error sources.

The differential sensitivity matrix, $[M_d]$, represents defects between the two inertial sensor axes. Before calibration, the disturbing term in equation (Eq. 10e) is evaluated with $|M_{dx}| = \sqrt{K_{dx}^2 + \theta_{dy}^2 + \theta_{dz}^2} = \sqrt{(10^{-2})^2 + 2 \times (10^{-3})^2} \approx 10^{-2}$. When the drag compensation system of the satellite is operating nominally, $\Gamma_{\text{app},c}(f_{ep})$ shall be limited to 10^{-12} m s^{-2} at the EP frequency. Considering the limit for each systematic error, 10^{-16} m s^{-2}, $|M_{dx}|$ needs to be inferior to 10^{-4} to reach the required mission accuracy.

In order to decrease $|M_{dx}|$ down to 10^{-4}, θ_{dy} and θ_{dz} have to be known to 1% and K_{dx} to 1.5%. The table below summarizes the MICROSCOPE instrument parameters to be considered in this approach and their values predicted by design. It also gives the amplitude of the induced disturbing effect on the EP test. The objectives for the in-orbit calibration of each parameter are also mentioned as well as the resulting residual effect on the test (Pradels, 2003).

Parameters	Maximal value per design	Impact before calibration (m s^{-2})	Specification for $e = 5 \times 10^{-3}$	Impact after calibration (m s^{-2})
θ_{cy} ($\Delta_z \leqslant 20$ μm)	1.5×10^{-3} rad	2×10^{-16}	10^{-3} rad	1.7×10^{-16}
θ_{cz} ($\Delta_z \leqslant 20$ μm)	1.5×10^{-3} rad	2.6×10^{-16}	10^{-3} rad	1.7×10^{-16}
$K_{cx} \cdot \Delta_x$ and $K_{cx} \cdot \Delta_z$ ($dK_{cx} \leqslant 10^{-2}$)	20.2 μm	4.15×10^{-14}	0.1 μm	2.1×10^{-16}
Δ_y ($\theta_{cz} = 1.5 \times 10^{-3}$ rad)	20 μm	3.4×10^{-16}	0.4 μm	6.8×10^{-18}
K_{dx}	10^{-2}	10^{-14}	1.5×10^{-4}	1.5×10^{-16}
θ_{dy} and θ_{dz}	10^{-3} rad	2×10^{-15}	5×10^{-5} rad	10^{-16}
Total		9.8×10^{-14}		1.1×10^{-15}

We can see that the total contribution is inferior to the signal to be detected but the repartition is not equivalent between each parameter. Indeed, some parameters are more easily calibrated than others. An optimisation of the repartition of the contribution could improve the global correction of the measurement.

5. The calibration

In order to correct the detected signal, each parameter mentioned in the previous table is calibrated in orbit by taking advantage of the drag-free system to apply periodic accelerations on the instrument, at well-known frequencies about or along the instrument axes.

From the equations of satellite motion and of the instrument measurement, calibration procedures are determined. For each parameter, the amplitudes of the necessary calibrating signals have been determined taking into account the capabilities of the satellite propulsion system and the required signal to noise ratio in the calibration data processing. The duration of each calibration session is a trade-off between the interest to limit the overall calibration phase duration (in order to allow more alternating calibration and EP test phases during the mission) and the interest to increase the rejection of the stochastic errors during the calibration (to be compared to the systematic errors).

The minimum session duration, provided hereafter for each parameter, is simply evaluated by

$$T_{\text{meas}} = \left(\frac{\text{Stoc}}{\text{Spec} - \text{Sys}}\right)^2, \tag{11}$$

where Stoc represents the stochastic error of the signal, Sys the systematic error at the frequency of the calibration and Spec the amplitude of the signal to be detected according to the specification. T_{meas} is also considered to be at least one orbit period, i.e. about 6000 s at the considered 730 km altitude, the disturbing signals appearing at the orbital frequency harmonics being in that way better rejected.

5.1. Calibration of the offcentrings between the two test-masses

The Earth's gravity gradient induces a major signal in the differential measurement at twice the test frequency f_{ep}. An estimate of Δ_x and Δ_z can be obtained from this well characterized signal with a sufficient accuracy.

$$K_{cx} \cdot \Delta_x \approx \frac{1}{T_{xx}(2f_{ep})} \cdot (2 \cdot \Gamma_{\text{meas},dx}(2f_{ep}) + \theta_{cy} \cdot \Delta_z \cdot T_{zz}(2f_{ep}) + \Gamma_{n,dx}(2f_{ep})) \tag{12}$$

In this case, the systematic error (due to $\theta_{cy} \cdot \Delta_z = 1.5 \times 10^{-3} \cdot 2 \times 10^{-6}$) corresponds to 0.03 μm and the statistic error (due to the measurement noise) is $5\ \mu\text{m}/\sqrt{\text{Hz}}$. $K_{cx} \cdot \Delta_x$ calibration requires at least $T_{\text{meas}} = 5100$ s, or nearly two orbits including margin of one additional orbit.

Δ_z also needs two orbits for its evaluation. The advantage of the method of calibration of these parameters is the fact that they can be estimated during the mission without any specific motion of the satellite or instrument.

That is not the case for Δ_y, which is evaluated by oscillating the satellite around the x or z axis. The angular acceleration of the satellite is limited to $2 \times 10^{-6}\ \text{rad s}^{-2}$ by the maximum thrust available from the propulsion system. In Eq. (13), an oscillation about z has been selected:

$$\Delta_y \approx \frac{2}{\dot{\omega}_z} \cdot [(1 - dK_{cx}) \cdot \Gamma_{\text{meas},dx}(f_{\text{calib}}) - \theta_{cz} \cdot \Gamma_{\text{app},dy}(f_{\text{calib}}) - \theta_{cy} \cdot \Gamma_{\text{app},dz}(f_{\text{calib}}) - M_{dx} \cdot \Gamma_{\text{app},c}(f_{\text{calib}}) + \Gamma_{n,d}(f_{\text{calib}})] \tag{13}$$

The systematic error is evaluated to 0.04 μ (due to $\frac{2}{\dot{\omega}_z} \cdot \theta_{cz} \cdot \Gamma_{\text{app},dy}(f_{\text{calib}}) = 0.03$ μm and $\frac{2}{\dot{\omega}_z} \cdot M_{dx} \cdot \Gamma_{\text{app},c}(f_{\text{calib}}) = 0.01$ μm). The statistic error is $3\ \mu\text{m}/\sqrt{\text{Hz}}$, due to the measurement noise. According to Eq. (11), $T_{\text{meas}} = 70$ s, leading to one orbit session. When considering the evaluation of all three offcentring components by oscillating the satellite, six orbits are necessary.

5.2. Calibration of the common misalignments

To estimate the off-diagonal components of the common sensitivity matrix, i.e. the attitude angles between the instrument axes and the satellite star tracker reference, the satellite is again oscillated about one reference axis (x or y), with a maximal angular acceleration of $2 \times 10^{-6}\ \text{rad s}^{-2}$ and a frequency of f_{sat}. This oscillation is produced by biasing the star sensor output to be sure that the oscillation is obtained in the satellite frame and not in the instrument one. The drag-free system has to be used in the bandwith of the star tracker functioning (Pradels, 2003).

Simultaneously, the test-masses of the instrument are moved along the axial direction (z axis) with a 10 μm sine amplitude at a frequency f_{instr}. The combination of both motions highlights Coriolis terms, which are neglected in Eq. (4) when both masses are controlled relatively motionless with an accuracy of at least 10^{-11} m. The axes of oscillation have been chosen from a numerical analysis in order to decrease the tone error as much as possible.

$$\theta_{cy} \approx \frac{2 \cdot ([M_{dx}] \cdot \vec{\Gamma}_{\text{app},c}(f_{\text{cal}}) - \Gamma_{\text{meas},dx}(f_{\text{cal}})) + \Gamma_{n,dx}(f_{\text{cal}})}{\dot{\omega}_z \cdot \Delta_{x/y}/2 + \omega_z \cdot \dot{\Delta}_{x/y}} \tag{14}$$

In the same way

$$\theta_{cz} \approx \frac{2 \cdot ([M_{dx}] \cdot \vec{\Gamma}_{\text{app},c}(f_{\text{cal}}) - \Gamma_{\text{meas},dx}(f_{\text{cal}})) + \Gamma_{n,dx}(f_{\text{cal}})}{\dot{\omega}_z \cdot \Delta_{x/y}/2 + \omega_z \cdot \dot{\Delta}_{x/y}} \tag{15}$$

The component of the measurement at $f_{\text{cal}} = f_{\text{instr}} - f_{\text{sat}}$ is about $2 \times 10^{-13}\ \text{m s}^{-2}$, to be evaluated with a precision of $10^{-13}\ \text{m s}^{-2}$.

Considering only the resolution of the instrument ($10^{-12}\ \text{m s}^{-2}/\sqrt{\text{Hz}}$, which corresponds to a statistic

equivalent error on θ_{cy} of 0.03 rad/rad/$\sqrt{\text{Hz}}$), the required calibration duration is only 100 s and the systematic error is evaluated to 1.3×10^{-4} rad. The calibration for this misalignment has to last about $T_{\text{meas}} = 1200$ s, leading to one orbit for one angle evaluation. By selecting other satellite axes of rotation, the same angle can be measured in two ways, increasing the confidence in the calibration. Eight orbits (including margins) are presently considered for the evaluation of these two common angles.

5.3. Calibration of the mismatching and misalignments between both sensors

For the evaluation of the mismatching and misalignments between both sensor axes of the same SAGE instrument, the linear acceleration of the satellite is modulated by a sine wave. The statistical error is due to the instrument noise level and has a value of $1.5 \times 10^{-4}/\sqrt{\text{Hz}}$. The scale factor ($K_{dx}$) systematic error is 1.2×10^{-4}. For the calibration objectives of 1.5×10^{-4}, the session duration is $T_{\text{meas}} = 25$ s, so one orbit.

For the misalignment angles, θ_{dy} and θ_{dz}, the 5×10^{-5} rad objective of accuracy is reached with systematic error of 3×10^{-5} rad and a calibration session of $T_{\text{meas}} = 56$ s, so again one orbit for each angle.

Three orbits are then needed for the calibration of $[M_{dx}]$, or six orbits when adding an extra orbit of margin to each session.

The table below sums up the parameters to be calibrated, their specification, the time needed to achieve this specification and their contribution after calibration.

Parameters	Specification	Calibration duration (orbits)	Performance (m s^{-2})
θ_{cy}	10^{-3} rad	4	1.7×10^{-16}
θ_{cz}	10^{-3} rad	4	1.7×10^{-16}
$K_{cx} \cdot \Delta_x$	0.1 μm	2	2.1×10^{-16}
$K_{cx} \cdot \Delta_z$	0.1 μm	2	2.1×10^{-16}
Δ_y	0.4 μm	5	6.8×10^{-18}
K_{dx}	1.5×10^{-4}	2	1.5×10^{-16}
θ_{dy}	5×10^{-5} rad	2	10^{-16}
θ_{dz}	5×10^{-5} rad	2	10^{-16}
Total		23	1.1×10^{-15}

The calibration will take place before and after each measurement phase in order to detect drifts of the parameters that may occur. Even if the parameters could be calibrated on ground, an in-flight calibration would be necessary to check their stability after the launch.

6. Conclusion

In-orbit calibration of the science instrument is mandatory to achieve the targetted accuracy of 10^{-15} for the Equivalence Principle test. This calibration phase is in fact one of the major elements of the space mission. Sensitivities of the electrostatic accelerometers and orientations of the axes, with respect to each other or with respect to the satellite star tracker, can be evaluated by softly oscillating the satellite in attitude or in translation. The offcentring between the test-masses can be observed in the same way in addition to the evaluation performed via the Earth gravity gradient signals. The required precise motions of the satellite but also of the masses can be produced by the FEEP electrical thrusters, while similar motions of the masses are provided by the electrostatic actuators around the masses. Calibration sessions have been established to evaluate the possibilities offered by the satellite and the instrument operation. The minimum duration of each session devoted to the evaluation of each parameter has been computed and the first calibration scenario requires 23 orbits for one SAGE instrument leading to about three days for both of them. The drag-free point of the satellite will be centered on the SAGE mass being calibrated.

Quadratic effects are not taken into account in this article but need to be studied as well as the other parameters presented. The contribution cannot be equally allocated between all the parameters, as initially expected. An optimisation between them is necessary to decrease as much as possible the total disturbing harmonic error of the measurement.

Numeric simulations are being performed to validate the analytical calculations presented here and especially to take into account any thermal fluctuations during or between the calibration sessions.

Acknowledgements

The authors want to acknowledge the CNES MICROSCOPE team for discussions on the satellite operation, and Gilles Métris and Philippe Bério of OCA (Nice, France) for their support.

References

Anza, S., Armano, M., Balaguer, E., Benedetti, M., Boatella, C., Bosetti, P., Bortoluzzi, D., Brandt, N., Braxmaier, C., Caldwell, M., Carbone, L., Cavalleri, A., Ciccolella, A., Cristofolini, I., Cruise, M., Da Lio, M., Danzmann, K., Desiderio, D., Dolesi, R., Dunbar, N., Fichter, W., Garcia, C., Garcia-Berro, E., Garcia Marin, A.F., Gerndt, R., Gianolio, A., Giardini, D., Gruenage, R., Hammesfahr, A., Heinze, G., Hough, J., Hoyland, D., Hueller, M., Jennrich, O., Johann5, U., Kemble, S., Killow, C., Kolbe, D., Landgraf, M., Lobo, A., Lorizzo, V., Mance, D., Middleton, K., Nappo, F., Nofrarias, M., Racca, G., Ramos, J., Robertson, D., Sallusti, M., Sandford, M., Sanjuan, J., Sarra, P., Selig, A., Shaul, D., Smart, D., Smit, M., Stagnaro, L., Sumner, T., Tirabassi, C., Tobin, S., Vitale, S., Wand, V., Ward, H., Weber, W.J., Zweifel, P. The LTP experiment on the LISA Pathfinder mission. Class Quantum Gravity 22, 125–138, 2005.

Baessler, S., Heckel, B.R., Adelberger, E.G., Gundlach, J.H., Schmidt, U., Swanson, H.E. Improved Test of The Equivalence Principle for Gravitational Self-Energy. Phys. Rev. Lett. 83 (18), 3585–3588, 1999.

Dittus, H., Mehls, C. A new experiment baseline for testing the weak equivalence principle at the Bremen drop tower. Class Quantum Gravity 18, 2417–2425, 2001.

Einstein, A. Über das relativitätsprinzip und die aus demselben gezogenen folgerungen. Jahrbuch Radioaktivität Elektron. 4, 411–462, 1907.

Nordtvedt, K. Direct testing the equivalence principle with laser ranging to the moon. Adv. Space Res. 32 (7), 1311–1320, 2003.

Pradels, G. Étalonnage en orbite d'accéléromètres ultrasensibles pour un test du Principe d'Équivalence à 10^{-15}, PhD Thesis, Université Paris VI Pierre et Marie Curie, 2003.

Touboul, P., Rodrigues, M., Métris, G., Tatry, B. MICROSCOPE, testing the equivalence principle in space, C. R. Acad. Sci. Paris, T. 2, Série IV, pp. 1271–1286, 2001.

Touboul, P., Rodrigues, M. The MICROSCOPE space mission. Class Quantum Gravity 18, 2487–2498, 2001.